JOURNAL OF SPACECRAFT AND ROCKETS
Vol. 44, No. 3, May–June 2007

Theoretical and Numerical Study of Free-Molecular Flow Problems

Chunpei Cai*
ZONA Technology Inc., Scottsdale, Arizona 85258
and
Iain D. Boyd†
University of Michigan, Ann Arbor, Michigan 48109

DOI: 10.2514/1.25893

By using two velocity direction-position relations, we investigate free-molecular effusion flows out of a two-dimensional slit with a nonzero average exit velocity and a free-molecular effusion flow out of an annular slit with a zero average exit velocity. This study yields two sets of exact solutions and expressions for number density and velocity distributions in front of the exits. These solutions include the exact exit geometry parameters. Several properties of the solutions are discussed mathematically and physically. Numerical simulation results obtained with the direct simulation Monte Carlo method validate the analytical solutions. In general, the comparisons between analytical and numerical results are virtually identical. Besides the theoretical significance, the methodology used in this study can be further applied to study more realistic plume flows.

Nomenclature

d	=	atomic radius
f	=	velocity distribution function
H	=	semiheight for a 2-D slit
h	=	y coordinate for a point on a 2-D slit
Kn	=	Knudsen number
n	=	number density
R	=	inner and outer radii for an annulus, universal gas constant
U, V, W	=	macroscopic velocity
u, v, w	=	microscopic velocity
X, Y, Z	=	a point in front of the exit
X_*	=	a specific position on the centerline passing an annulus
β	=	$1/(2RT)$
γ	=	specific heat ratio
λ	=	mean free path
κ	=	ratio of R_2/R_1
θ	=	specific solid angle, one component for a polar coordinate
Ω	=	integral domain in velocity space

Subscript

o	=	averaged property at exit

I. Introduction

FREE-MOLECULAR flows passing through small holes represent fundamental and important problems in real applications such as materials processing in high vacuum chambers [1], spacecraft design [2], and metrology of gas flow [3]. Several investigators have proposed analytical expressions for the mass flow rate near the free-molecular regime in the case of gas flow from an orifice expanding into vacuum. For example, Liepmann [4] reported the efflux of gases through circular apertures, which is an example of a transition from the gasdynamic to the gaskinetic regime. Narasimha [5–7] further obtained the exact solutions of density and velocity distributions for a free-molecular effusion flow, and the results for a nearly free-molecular effusion flow, expanding into vacuum through a circular orifice. Brook [8] reported the density field of directed free-molecular flow from an annulus, to study the gas leakage effect from a spacecraft hatch. Recently, a detailed numerical study of rarefied gas flow through a thin orifice was reported [9].

In aerospace engineering, plume flows exhausted from electric propulsion devices are of current research interest. This study is an initial attempt to analytically investigate such plume flows. Electric propulsion systems such as Hall thrusters have several advantages over traditional chemical thrusters, and they are designed to operate in space for purposes of primary propulsion and on-orbit applications such as stationkeeping. For electric thrusters, their plume flows are of major interest for several reasons: First, plume flows can be used to study the performance of a thruster. Second, plume impingement on a spacecraft can have significant adverse effects.

There are many experimental measurements and numerical simulations of plasma plumes of electric thrusters, but there are very few reports of analytical studies in the literature. Most related previous kinetic work in the literature was concentrated on free-molecular flows out of a simplified geometry such as an orifice [5], and most studies concentrated on effusion flows with a zero average exit velocity, $U_0 = 0$. Obviously, further analytical results of the plume flowfield with more detailed thruster geometries, or nonzero average exit velocity, can provide new insights and aid the understanding of the plume flows out of electric thrusters.

Although there are several fundamental aspects of a plume flow out of an electric thruster, this study considers a few primary features. The fundamental features are as follows. First, most electric propulsion plume flows are almost free-molecular. The mean free path for gas propellant out of a thruster can be estimated with the following equation for the hard sphere collision model, $\lambda = 1/(\sqrt{2}\pi d^2 n_0)$, where d is the atomic diameter and n_0 is the reference number density. With a typical number density of 5×10^{18} m^{-3} at the exit of a Hall thruster, the mean free path for xenon is 0.268 m, which is wider than a typical Hall thruster acceleration channel. Second, the average velocity at a thruster exit plane is greater than zero. The average neutral speed at the thruster exit plane is usually sonic, and the average ion speed is always supersonic due to

Presented as Paper 3800 at the 9th AIAA/ASME Joint Thermophysics and Heat Transfer Conference, San Francisco, CA, 6–8 June 2006; received 22 June 2006; revision received 5 December 2006; accepted for publication 13 December 2006. Copyright © 2007 by Chunpei Cai. Published by the American Institute of Aeronautics and Astronautics, Inc., with permission. Copies of this paper may be made for personal or internal use, on condition that the copier pay the $10.00 per-copy fee to the Copyright Clearance Center, Inc., 222 Rosewood Drive, Danvers, MA 01923; include the code 0022-4650/07 $10.00 in correspondence with the CCC.

*Computational Fluid Dynamics Specialist, 9489 East Ironword Square Drive, previously Graduate Student Research Assistant, Department of Aerospace Engineering, University of Michigan, Ann Arbor, Michigan. Senior Member AIAA.

†Professor, Department of Aerospace Engineering, 1320 Beal Avenue. Associate Fellow AIAA.

electrostatic acceleration inside the thruster. Third, electric-field effects in the plume are important for ions. Fourth, collisions are important because they change the density and velocity distributions, but collisions happen rarely because the flow is almost free-molecular. Fifth, the ions are also accelerated rapidly inside the thruster, leading to plume divergence. To include all of these features in one step is unrealistic, and as an initial effort, by neglecting the primary features 3, 4, and 5 (i.e, the electric field), all collision effects, and the plume divergence, this paper investigates two different free-molecular gas flows out of a two-dimensional slit and an annular exit. The exact solutions to the two problems provide first-order approximations to cold plume flows, and they provide foundations to investigate new cases in a future study.

In the rest of this study, Sec. II presents the problems to be studied and a general solution method, Secs. III and IV present two free-molecular flow problems and their analytical solutions, Sec. V compares the results with particle simulation results, and Sec. VI summarizes this study.

II. Free-Molecular Flow Problems and General Treatment

The flows considered in this study are two problems of free-molecular gas flows out of an exit into vacuum:

1) In a two-dimensional thin slit with a width of $2H$, the average exit velocity U_0 is greater than zero.

2) In an annulus characterized by an inner radius R_1 and an outer radius R_2, the average exit velocity U_0 is zero.

This study adopts the following coordinate systems. Denote the plume direction as the X-axis direction, the direction normal to the X axis as the Y-axis direction, and the middle point of the slit/annulus center is the origin. The objective of this study is to obtain the analytical plume field flow solutions, especially the number density and velocities at any point downstream of the exit. Suppose the gas at the exit is in equilibrium with a uniform static temperature T_0 and a uniform number density n_0. Although the plume itself is in a highly nonequilibrium state, it is reasonable to assume that the flow is at equilibrium before it escapes from the exit. Using T_0 and n_0 to describe this equilibrium state is a natural selection, which was used by many researchers in the past.

A. General Methods

For a dilute gas flow at rest in equilibrium, the velocity distribution is described as a full Maxwellian distribution [10–12]. With a number density n_0 and a temperature T_0, the velocity distribution function at any point follows a Maxwellian distribution:

$$f(u,v,w) = n_0\left(\frac{\beta}{\pi}\right)^{3/2}\exp[-\beta(u^2+v^2+w^2)] \tag{1}$$

where $\beta = 1/2RT_0$. The highest velocity probability occurs at phase point $(u,v,w) = (0,0,0)$. For a velocity with a nonzero average value of U_0 along the X direction but a zero average value along the Y and Z directions, the distribution Eq. (1) is shifted along the U axis by a value of U_0.

With a known velocity distribution $f(u,v,w)$ at a point (X,Y,Z), the average number density normalized by a reference number density and velocities at (X,Y,Z) can be evaluated using the velocity distribution function [11]:

$$n(X,Y,Z) = \int_\Omega f(u,v,w)\,\mathrm{d}u\,\mathrm{d}v\,\mathrm{d}w \tag{2}$$

$$U(X,Y,Z) = \frac{1}{n(X,Y,Z)}\int_\Omega uf(u,v,w)\,\mathrm{d}u\,\mathrm{d}v\,\mathrm{d}w \tag{3}$$

$$V(X,Y,Z) = \frac{1}{n(X,Y,Z)}\int_\Omega vf(u,v,w)\,\mathrm{d}u\,\mathrm{d}v\,\mathrm{d}w \tag{4}$$

$$W(X,Y,Z) = \frac{1}{n(X,Y,Z)}\int_\Omega wf(u,v,w)\,\mathrm{d}u\,\mathrm{d}v\,\mathrm{d}w \tag{5}$$

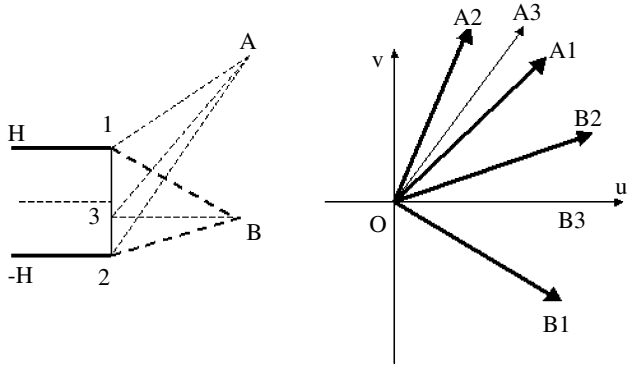

Fig. 1 Velocity spaces for points inside or outside of the plume core.

Hence, the critical step is to obtain the velocity distribution function and the integral domain in the velocity phase space. Narasimha [5] made an important observation for a free-molecular flow of gas escaping from an orifice, discussed next.

B. Observation

For any point (X,Y,Z) in front of the orifice, its velocity space can only have nonzero velocity within a specific solid angle Ω subtended by the specific point and exit edges:

$$f(u,v,w) = \begin{cases} n_0\left(\frac{\beta}{\pi}\right)^{3/2}\exp[-\beta(u^2+v^2+w^2)], & u,v,w \in \Omega; \\ 0, & u,v,w \notin \Omega \end{cases} \tag{6}$$

where $\beta = 1/2RT_0$ and Ω represents the integral domain in the velocity phase space. Figure 1 illustrates the velocity spaces for two points in front of the exit. One point, A, is outside the plume core region, whereas the other point, B, is inside the plume core. Velocity space A1-O-A2 represents the first point's integral domain, and B1-O-B2 represents the second point's integral domain. Line O-A3 represents the velocity contributed by particles starting from point 3, whereas the particle starting at point 3 that can arrive at point B is represented by the positive U axis.

Although this observation is critical, it is not enough to solve the high-speed plume flow, because the preceding fact about solid angles is not valid with a nonzero exit velocity U_0. To truly attack the free-molecular flows listed in this study, we believe it is necessary to reinterpret this fact with a deeper view as a velocity direction-position relation. From a given point on the exit, only particles with specific velocity components can arrive at a specific point (X,Y,Z) in front of the exit; on the other hand, if a particle's velocity direction satisfies this relation, then the particle must pass through the point in front of the thruster. Hence, this key velocity direction-position relation is a necessary and sufficient condition. This relation takes different forms in the two cases and will be illustrated later as Eqs. (7) and (13). These equations actually have three effects. First, they guarantee a one-to-one mapping relation between velocity phase spaces and provide a complete support to Eq. (6). Second, they can provide integral boundaries in the velocity space. Third, they may simplify the integral process by changing integral variables from velocities to geometry parameters of the exit.

III. Problem 1: Free-Molecular Flow Out of a Slit ($U_0 > 0$)

Narasimha [6] discussed the jet flow out of a point source with a nonzero average exit velocity. In this section, the finite semiwidth of slit H is considered. Consider the velocity space for a point (X,Y) in front of the slit. The velocity distribution at the point still follows Eq. (1), but the integral domain changes significantly because of the nonzero average exit velocity. With this change, from any point $(0,h)$ on the slit, particles can arrive at the point (X,Y) if, and only if, their velocity components (u,v) satisfy the following relation:

$$\tan(\theta) = \frac{Y-h}{X} = \frac{v}{u+U_0}, \qquad -H < y < H \tag{7}$$

To compare the difference in the integral domains for this case, the velocity distribution function does not shift to the right with a value of U_0. Hence, $u + U_0$ represents a particle's actual velocity along the X direction. Obviously, the nonzero average velocity U_0 does not destroy the one-to-one mapping relation between velocity phase spaces.

The nonzero values in the velocity space of point (X, Y) form a pie shape bounded by two lines from the slit edge points to the point (X, Y), and the number density and velocities at the point (X, Y) can be obtained by integrating the probability distribution function in the velocity phase within two lines, both starting from the origin point:

$$\theta_1 = \arctan\left(\frac{Y-H}{X}\right), \qquad \theta_2 = \arctan\left(\frac{Y+H}{X}\right) \tag{8}$$

With this simple integral domain in the velocity phase space, the integrals can be simplified with the following relation:

$$\mathrm{d}u\,\mathrm{d}v = \bar{V}\,\mathrm{d}\bar{V}\,\mathrm{d}\theta \tag{9}$$

where $\bar{V} = \sqrt{u^2 + v^2}$.

Figure 2 shows the effect of the nonzero exit velocity on the integral domain in velocity space. On the left side is a case of zero average exit velocity and the right side is a case of nonzero average exit velocity. In both plots, region Aoa represents an integral domain for a point (X, Y) out of the plume core ($|Y| > H$), and region Bob represents an integral domain for a point in the plume core ($|Y| < H$). The integral domain widens as the point (X, Y) becomes closer to the slit. It is immediately observed that there are several changes between these two integral domains. The existence of a nonzero U_0 translates the integral domain to the left, without any effects on the slopes of the two domain boundaries. The two boundaries shift up or down, resulting in different effects on the points inside the plume core ($|Y| < H$) and outside the plume core ($|Y| > H$). If the point is inside the core, then the number density increases for the case of a nonzero average exit velocity because of a larger integral domain including regions close to the origin with the highest probability, whereas the number density at a point outside the plume core decreases because the origin point is excluded from the integral domain. Physically, this is reasonable: With a higher average exit velocity, more particles are injected axially into the simulation domain, whereas there is less time for particles to diffuse vertically outside the core region, because they flow downstream quite quickly. Hence, a nonzero average exit velocity results in a higher density at points inside the plume core and a lower density at points outside the core region.

Note from Eq. (8) that $\theta_2 > \theta_1$, $0 < \theta_2 < \pi/2$, and $-\pi/2 < \theta_1 < \pi/2$, therefore, the number density and velocities at any point (X, Y) in front of the slit can be derived [13,14]. The final results are

$$n(X,Y) = \frac{\exp\left(-\beta U_0^2\right)}{2\pi}(\theta_2 - \theta_1) + \frac{1}{4}\left[erf(\sqrt{\beta}U_0\sin\theta_2) - \frac{\theta_1}{|\theta_1|}erf(\sqrt{\beta}U_0\sin|\theta_1|)\right] + \frac{\sqrt{\beta/\pi}}{2}\int_{\theta_1}^{\theta_2}\exp\left(-\beta U_0^2\sin^2\theta\right)U_0\cos\theta\, erf(\sqrt{\beta}U_0\cos\theta)\,\mathrm{d}\theta \tag{10}$$

$$\frac{U(X,Y)}{\sqrt{2RT_0}} = \frac{\exp\left(-\beta U_0^2\right)}{2n\pi\sqrt{2RT_0}} \times\left\{\int_{\theta_1}^{\theta_2}\left[\frac{\sqrt{\pi/\beta}}{2}\exp\left(\beta U_0^2\cos^2\theta\right)\cos\theta[1+erf(\sqrt{\beta}U_0\cos\theta)]\right]\mathrm{d}\theta + \frac{U_0(\theta_2-\theta_1)}{2} + \frac{U_0[\sin(2\theta_2)-\sin(2\theta_1)]}{4} + \sqrt{\beta\pi} \times\int_{\theta_1}^{\theta_2}\left[U_0^2\cos^3\theta[1+erf(\sqrt{\beta}U_0\cos\theta)\right]\exp\left(\beta U_0^2\cos\theta\right)\right]\mathrm{d}\theta\right\} \tag{11}$$

$$\frac{V(X,Y)}{\sqrt{2RT_0}} = \frac{1}{4\sqrt{\pi}n}\left\{\exp\left(-\beta U_0^2\sin^2\theta_1\right)\cos\theta_1[1+erf(\sqrt{\beta}U_0\cos\theta_1)] - \exp\left(-\beta U_0^2\sin^2\theta_2\right)\cos\theta_2[1+erf(\sqrt{\beta}U_0\cos\theta_2)]\right\} \tag{12}$$

This set of solutions includes two types of factors: geometry factors represented by θ_1 and θ_2 and other factors involving complex nonlinear relations with U_0, the average exit velocity at the slit.

From Eqs. (10–12), it can be proved that $n(X, -Y) = n(X, Y)$, $U(X, -Y) = U(X, Y)$, and $V(X, -Y) = -V(X, Y)$. These results can be obtained with aid from the fact that for points (X, Y) and $(X, -Y)$, the integral domains in velocity space are symmetric about the U axis.

Another interesting comparison is the quantities on the exit center and exit tip. Though it is difficult to obtain the exact values at these two points, the integral domain has some simple properties: On the exit center, the integral domain is from $-(\pi/2)$ to $\pi/2$, whereas on the exit tip, the integral domain is from 0 to $\pi/2$. Hence, it can be concluded from Eqs. (10) and (11) that the number density at the exit tip is half of the value at the exit center, whereas the velocity along the X direction has a uniform value.

IV. Problem 2: Free-Molecular Effusion Flow Out of an Annular Exit ($U_0 = 0$)

This free-molecular flow is not only applicable for the situation of effusion flows out of Hall thrusters, but also to estimate the flow out of a poorly sealed spacecraft hatch. Previously, Brook [8] reported the density field results, and in this study, we intend to give a complete set of results with velocity distributions.

For this case, the velocity direction-position relation takes a new format. Suppose that the average velocity at the circular exit is zero; from any point $(0, y, z)$ on the exit that is characterized by an internal radius of R_1 and an external radius of R_2, only particles with the following special velocity components can arrive at a point (X, Y, Z) in front of the exit:

$$\frac{X}{u} = \frac{Y-y}{v} = \frac{Z-z}{w} \tag{13}$$

where $X > 0$, $Y > 0$, and $Z > 0$. Combined with geometry relations

$$z = r\sin\theta = Z - Xw/u, \qquad y = r\cos\theta = Y - Xv/u \tag{14}$$

where $r \in [R_1, R_2]$, $\theta \in [0, 2\pi]$, the integrals for the number density and the velocities can be simplified using the following variable

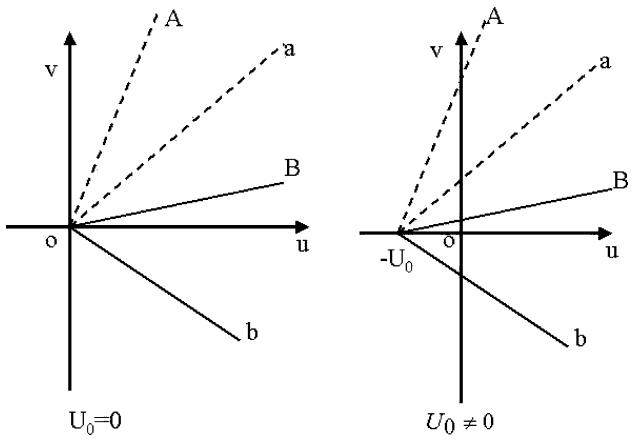

Fig. 2 Effect on velocity space by the average exit velocity.

change:

$$\mathrm{d}v\,\mathrm{d}w = \begin{vmatrix} \frac{\partial v}{\partial r} & \frac{\partial v}{\partial \theta} \\ \frac{\partial w}{\partial r} & \frac{\partial w}{\partial \theta} \end{vmatrix} \mathrm{d}r\,\mathrm{d}\theta = \frac{u^2}{X^2} r\,\mathrm{d}r\,\mathrm{d}\theta \tag{15}$$

By observing the integral domains, the free-molecular flow out of an annulus can be considered as a large circular source of radius R_2 minus a small circular sink of radius R_1.

The final results of number density and velocities at a point $(X, 0, Z)$ are

$$\begin{aligned} n(X,0,Z) = -\frac{X}{4\pi}\int_{-\pi}^{\pi}\Bigg[& \frac{\mathrm{d}\theta}{\sqrt{X^2+Z^2+R_2^2-2R_2Z\sin\theta}} \\ & - \frac{Z\sin\theta(R_2 - Z\sin\theta)\,\mathrm{d}\theta}{(X^2+Z^2\cos^2\theta)\sqrt{X^2+Z^2+R_2^2-2R_2Z\sin\theta}}\Bigg] \\ & + \frac{X}{4\pi}\int_{-\pi}^{\pi}\Bigg[\frac{\mathrm{d}\theta}{\sqrt{X^2+Z^2+R_1^2-2R_1Z\sin\theta}} \\ & - \frac{Z\sin\theta(R_1 - Z\sin\theta)\,\mathrm{d}\theta}{(X^2+Z^2\cos^2\theta)\sqrt{X^2+Z^2+R_1^2-2R_1Z\sin\theta}}\Bigg] \end{aligned} \tag{16}$$

$$\begin{aligned} \frac{U(X,0,Z)}{\sqrt{2RT_0}} = \frac{X^2}{2\pi n\sqrt{\pi}}\Bigg(& \frac{\pi}{\sqrt{\left(X^2+Z^2+R_1^2\right)^2 - 4R_1^2Z^2}} \\ & - \frac{\pi}{\sqrt{\left(X^2+Z^2+R_2^2\right)^2 - 4R_2^2Z^2}} \\ & + \int_{-\pi}^{\pi}\Bigg[\frac{Z\sin\theta(R_2 - Z\sin\theta)\,\mathrm{d}\theta}{2\left(X^2+Z^2+R_2^2-2R_2Z\sin\theta\right)(X^2+Z^2\cos^2\theta)} \\ & - \frac{Z\sin\theta(R_1 - Z\sin\theta)\,\mathrm{d}\theta}{2\left(X^2+Z^2+R_1^2-2R_1Z\sin\theta\right)(X^2+Z^2\cos^2\theta)} \\ & + \frac{Z\sin\theta\,\mathrm{d}\theta}{2(X^2+Z^2\cos^2\theta)^{3/2}}\arctan\frac{R_2 - Z\sin\theta}{\sqrt{X^2+Z^2\cos^2\theta}} \\ & - \frac{Z\sin\theta\,\mathrm{d}\theta}{2(X^2+Z^2\cos^2\theta)^{3/2}}\arctan\frac{R_1 - Z\sin\theta}{\sqrt{X^2+Z^2\cos^2\theta}}\Bigg]\mathrm{d}\theta\Bigg) \end{aligned} \tag{17}$$

$$\begin{aligned} \frac{W(X,0,Z)}{\sqrt{2RT_0}} = \frac{1}{2\pi n\sqrt{\pi}}\int_0^{2\pi}\Bigg[& \frac{-(Z/2)\cos(2\theta)\,\mathrm{d}\theta}{\left[X^2+R_2^2+Z^2-2R_2Z\sin\theta\right]} \\ & + \frac{(Z/2)\cos(2\theta)\,\mathrm{d}\theta}{\left[X^2+R_1^2+Z^2-2R_1Z\sin\theta\right]} \\ & - \frac{\sin(\theta)\,\mathrm{d}\theta}{\sqrt{X^2+Z^2\cos^2\theta}}\left(\arctan\frac{R_2 - Z\sin\theta}{\sqrt{X^2+Z^2\cos^2\theta}}\right. \\ & \left. - \arctan\frac{R_1 - Z\sin\theta}{\sqrt{X^2+Z^2\cos^2\theta}}\right) \\ & + \frac{\sin\theta(X^2+2Z^2\cos^2\theta)\,\mathrm{d}\theta}{2(X^2+Z^2\cos^2\theta)^{3/2}}\left(\arctan\frac{R_2 - Z\sin\theta}{\sqrt{X^2+Z^2\cos^2\theta}}\right. \\ & \left. - \arctan\frac{R_1 - Z\sin\theta}{\sqrt{X^2+Z^2\cos^2\theta}}\right) \\ & + \frac{\sin\theta(X^2+2Z^2\cos^2\theta)(R_2 - Z\sin\theta)\,\mathrm{d}\theta}{2(X^2+Z^2\cos^2\theta)\left(X^2+Z^2+R_2^2-2R_2Z\sin\theta\right)} \\ & - \frac{\sin\theta(X^2+2Z^2\cos^2\theta)(R_1 - Z\sin\theta)\,\mathrm{d}\theta}{2(X^2+Z^2\cos^2\theta)\left(X^2+Z^2+R_1^2-2R_1Z\sin\theta\right)}\Bigg] \end{aligned} \tag{18}$$

From the preceding relations, the centerline variations are

$$\begin{aligned} n(X,0,0) &= \frac{X}{2\sqrt{X^2+R_1^2}} - \frac{X}{2\sqrt{X^2+R_2^2}} \\ \frac{U(X,0,0)}{\sqrt{2RT_0}} &= \frac{X}{\sqrt{\pi}}\left(\frac{1}{\sqrt{X^2+R_1^2}} + \frac{1}{\sqrt{X^2+R_2^2}}\right) \end{aligned} \tag{19}$$

Obviously, when X changes from 0 to ∞, the centerline number density increases from 0 to a specific value, then decreases slowly to zero, whereas the speed ratio $U(X,0,0)/\sqrt{2RT_0}$ increases from 0 to $2/\sqrt{\pi}$.

V. Simulations and Discussions

Although the preceding results involve several integral terms that cannot be explicitly removed, numerical evaluations are convenient via a computer. The subroutine for the error function can be found in any numerical computing book [15].

Because the flows are rarefied, it is appropriate to compute them using the direct simulation Monte Carlo (DSMC) method [10]. In this study, we used a specific DSMC package named MONACO [16] to perform the validation simulations. The simulation domain and mesh are quite simple, and the collision function in MONACO is turned off. Under this situation, the value of the number density at the exit does not produce any difference in the final result, and an exact free-molecular flow is guaranteed.

First, consider the high-speed flow passing through a 2-D slit. The existence of a nonzero average exit velocity has a significant effect on the flowfield. If the exit average velocity $U_0 = 0$, then the boundary line between the flowfield and a vacuum is the vertical line above the slit. When the average exit velocity increases, the boundary line begins to decline toward the plume core, though it still starts with the upper tip $(0, H)$. Hence, there will be a larger void region connected with point $(0, H)$ and residing above the slit. This presents a problem for evaluation of the analytical results, because the number density is a component of the denominators in the velocities expressions, and in the analytical vacuum region, the numerical error may exceed the small analytical magnitudes of the number densities. For simulation results from the DSMC method, this is not a problem, because the evolution of velocities does not involve a denominator of number density. For the analytical solutions to the slit problem, an effective boundary line of $n/n_0 = 0.0001$ is introduced to represent the plume edge, and the comparisons are restricted to areas within this boundary. Figure 3 shows several such effective boundary lines with different average exit velocities at the slit. It indicates that as the average exit velocity increases, the plume region narrows because particles have less time to diffuse vertically. When the exit speed is high enough, the flowfield is confined to a narrow region close to the plume core.

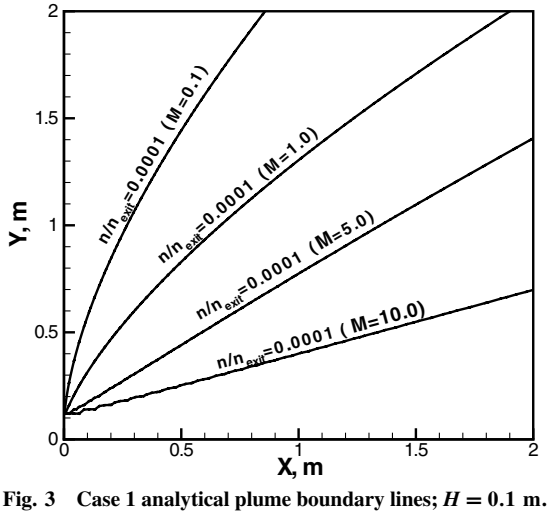

Fig. 3 Case 1 analytical plume boundary lines; $H = 0.1$ m.

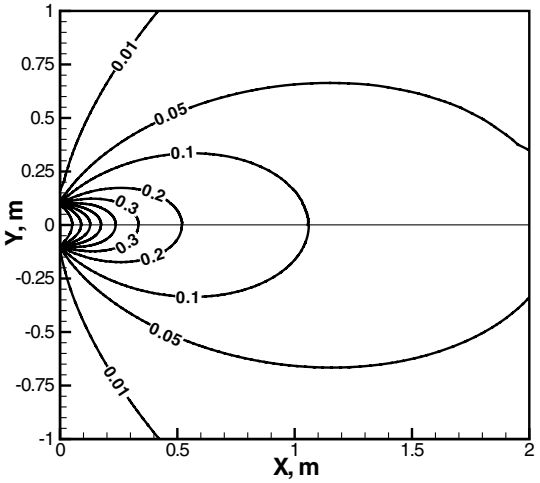

Fig. 4 Case 1 contours of $n(X, Y)$; $H = 0.1$ m and $U_0 = \sqrt{\gamma RT_0}$; DSMC (top) and analytical (bottom).

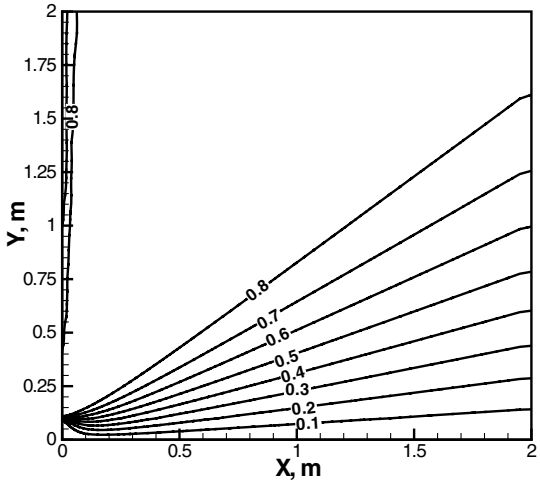

Fig. 6 Case 1 contours of $V(X, Y)/\sqrt{2RT_0}$; DSMC; $H = 0.1$ m and $U_0 = \sqrt{\gamma RT_0}$).

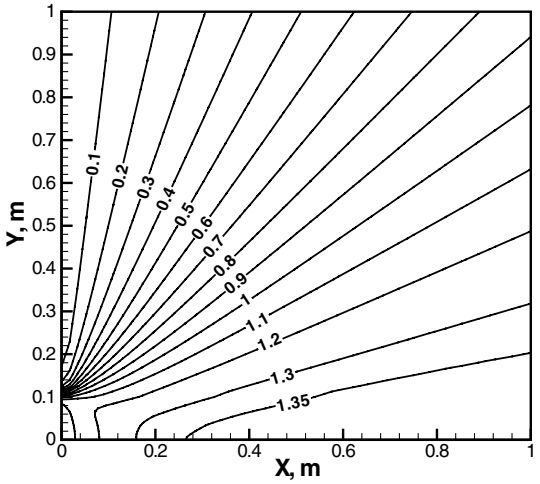

Fig. 5 Case 1 contours of $U(X, Y)/\sqrt{2RT_0}$; DSMC; $H = 0.1$ m and $U_0 = \sqrt{\gamma RT_0}$).

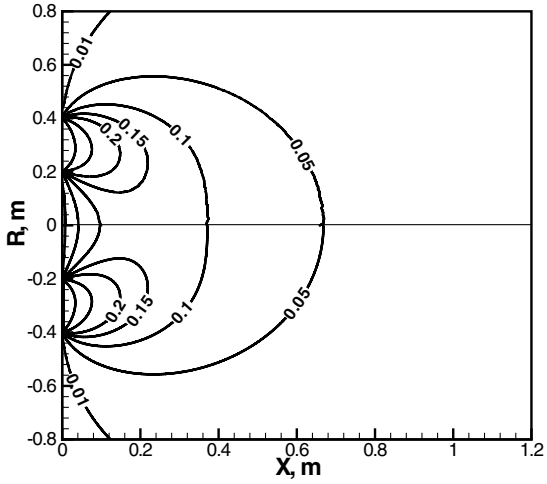

Fig. 7 Case 2 contours of normalized number density; $R_1 = 0.2$ m, $R_2 = 0.4$ m, and $U_0 = 0$; DSMC (top) and analytical (bottom).

Figure 4 shows a comparison of number density contours with the DSMC results for a slit with a semiheight of $H = 0.1$ m. The average exit velocity at the slit is the sonic speed. The exit temperature is set to $T = 300$ K. By turning off the collision function in the DSMC method, the results are expected to be close to free-molecular. Generally, the comparison shows almost identical results.

Figures 5 and 6 show the corresponding simulation results of velocity contours. Because of the singularity problem mentioned earlier, the analytical results are not valid beyond the boundary line; hence they are omitted here. It can be observed that the flow patterns have a narrow zone in which exit effects dominate, but in the far field, the contour lines are straight.

An axisymmetric DSMC simulation without collisions is performed to validate the analytical results for the annular flows. The inner and outer radii of the annulus are set to $R_1 = 0.2$ m and $R_2 = 0.4$ m, respectively. About 19,200 rectangular cells are used to represent a square simulation domain of 1.2 by 1.2 m. As before, the temperature at the exit is set to 300 K.

Figure 7 shows the contours of number density; the bottom contours are the analytical results and the top contours represent the DSMC results. In the whole simulation domain, the comparison shows almost identical results. Figures 8 and 9 show the contours of velocities. Both comparisons are quite satisfactory, as well. In all three results, both the exit region and the slow "cavity" region in the center, which is characterized by negative W_z, are clearly captured. There are two branches of zero-value lines for W_z: one is along the X axis, whereas the other curved branch starts from a point inside the exit and ends on the X axis. The intersection point of the two branches can be found analytically from Eqs. (18), on the specific point

$$\left.\frac{\partial W(X, 0, Z)}{\partial Z}\right|_{Z=0} = 0 \tag{20}$$

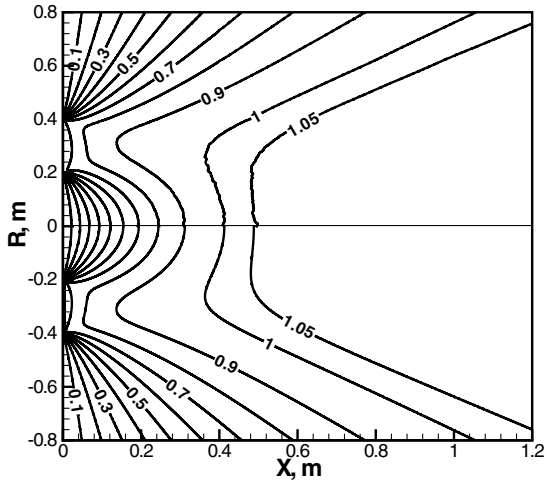

Fig. 8 Case 2 contours of $U(X, 0, R)/\sqrt{2RT_0}$; $R_1 = 0.2$ m, $R_2 = 0.4$ m, and $U_0 = 0$; DSMC (top) and analytical (bottom).

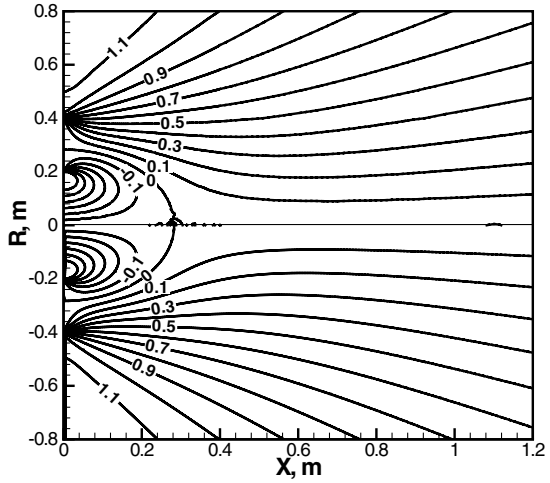

Fig. 9 Case 2 contours of $W(X,0,R)/\sqrt{2RT_0}$; $R_1 = 0.2$ m, $R_2 = 0.4$ m, and $U_0 = 0$; DSMC (top) and analytical (bottom).

From this condition, it is straightforward to show that $X = \sqrt{R_1 R_2}$ is the intersection point on the axis.

Another important result is obtained for the location on the axis for which the highest number density occurs. From Eq. (16),

$$\frac{\partial n(X,0,0)}{\partial X} = \frac{\partial}{\partial X}\left(\frac{X}{2\sqrt{X^2+R_1^2}} - \frac{X}{2\sqrt{X^2+R_2^2}}\right) = 0 \qquad (21)$$

This leads to

$$X_* = \sqrt{\frac{R_2^2 R_1^{4/3} - R_1^2 R_2^{4/3}}{R_2^{4/3} - R_1^{4/3}}} = \frac{R_1^{2/3} R_2^{2/3}}{\sqrt{R_1^{2/3} + R_2^{2/3}}} = \frac{\kappa^{2/3} R_1}{\sqrt{1+\kappa^{2/3}}} \qquad (22)$$

$$n_{\max} = \tfrac{1}{2}(\kappa^{2/3} - 1)(1 + \kappa^{2/3} + \kappa^{4/3})^{-1/2} \qquad (23)$$

where $\kappa = R_2/R_1 > 1$. Further notice that Eq. (22) is an increasing function of κ, therefore a range of X_* can be determined as

$$R_1/\sqrt{2} < X_* < \kappa^{1/3} R_1 = \left(R_1^2 R_2\right)^{1/3} < \frac{2R_1 + R_2}{3} \qquad (24)$$

It is interesting to notice that this distance is less than the average value of the inner and outer radius.

Equations (22) and (23) contain only the inner radius and outer radius of the annulus. This is because the derivation is based on a free-molecular flow assumption without collision effects, hence the final expression contains only geometry factors, which is quite expected and reasonable. For an annulus with $R_1 = 0.2$ m and $R_2 = 0.4$ m, the highest number density along the centerline is 0.1299 at $X = 0.196$ m. The DSMC simulation without collisions predicts the same value at the same location.

VI. Conclusions

In this study, two fundamental free-molecular flows out of an exit with different geometries were investigated analytically and validated by particle simulations. The important velocity-position relations, Eqs. (7) and (13), provided one-to-one mapping relations between velocity spaces for a specific point in front of the exit and a point on the exit. These two relations validated Eq. (6) and provided integral domains for both problems.

This study yielded analytical exact solutions or exact expressions for detailed exit geometries. The first problem was of significant importance, because it is the case closest to realistic plume flows. The analytical results of the first problem indicated that the solutions were composed of two factors: one factor representing simple geometry relations and the other factor representing complex nonlinear effects from the average exit velocity at the slit. The second case belongs to a category of true effusion problems with a zero average exit velocity. Its flowfields were associated with geometry factors and no collisions effects were considered. These results included accurate geometry factors, hence they were expected to yield more accurate results than existing models in the literature. These analytical results clearly captured all features of the whole flowfield.

Two particle simulations were performed with the DSMC method to validate the analytical solutions obtained in this study, and in these simulations, the collision functions were turned off. Generally, simulations for these two cases yield good agreement with the analytical results and most of the results are essentially identical, and all detailed flow structures are captured successfully. It can be concluded that the general treatment of these two free-molecular flows from different exit shapes are valid.

This study is an initial effort to seek analytical results to describe the free-molecular plume flows from electric propulsion thrusters. It provided a solid basis for further analytical studies such as plume flows out of a circular or annular thruster with a nonzero average velocity at the thruster exit.

To keep this paper concise, the lengthy and complex derivation process are omitted. More details of these two cases and another four different cases of free-molecular flows can be found in [13].

Acknowledgment

The authors gratefully acknowledge funding for this work from the U.S. Air Force Office of Scientific Research under grant FA9550-05-1-0042. This work was carried out and completed at the University of Michigan.

References

[1] Aktas, O., Aluru, N. R., and Ravaioli, U., "Application of a Parallel DSMC Technique to Predict Flow Characteristics in Microfluidic Filters," *Journal of Microelectromechanical Systems* Vol. 10, No. 4, 2001, pp. 538–549.

[2] Jamison, A. J., Ketsdever, A. D., and Muntz, E. P., "Gas Dynamic Calibration of a Nano-Newton Thrust Stand," *Review of Scientific Instruments* Vol. 73, No. 10, 2002, pp. 3629–3673.

[3] Szwemin, P., Szymanski, K. H., and Jousten, S., "Monte Carlo Study of a New PTB Rrimary Standard for Very Low Pressure," *Metrologia*, Vol. 36, No. 1, 1999, pp. 562–564.

[4] Liepmann, H. W., "Gas Kinetics and Gasdynamics of Orifice Flow," *Journal of Fluid Mechanics*, Vol. 10, No. 1, 1961, pp. 65–79.

[5] Narasimha, R., "Orifice Flow of High Knudsen Number," *Journal of Fluid Mechanics* Vol. 10, No. 3, 1961, pp. 371–384.

[6] Narasimha, R., "Collisionless Expansion of Gases into Vacuum," *Journal of Fluid Mechanics*, Vol. 12, No. 3, 1962, pp. 294–308.

[7] Narasimha, R., "Some Flow Problems in Rarefied Gas Dynamics," Ph.D. Thesis, California Inst. of Technology, Pasadena, CA, 1961.

[8] Brook, J. W., "Density Field of Directed Free-Molecular Flow from an Annulus," *Journal of Spacecraft and Rockets*, Vol. 6, No. 6, 1969, pp. 755–757.

[9] Sharipov, F., "Numerical Simulation of Rarefied Gas Flow Through a Thin Orifice," *Journal of Fluid Mechanics*, Vol. 518, No. 1, 2004, pp. 35–60.

[10] Bird, G. A., *Molecular Gas Dynamics and the Direct Simulation of Gas Flows,* Oxford Univ. Press, New York, 1994.

[11] Gombosi, T. I., *Gaskinetic Theory*, Cambridge Univ. Press, New York, 1994.

[12] Vincenti, W. G., and Kruger, C. H., *Introduction to Physical Gas Dynamics*, Krieger Publishing, Malabar, Florida, 1986.

[13] Cai, C., "Theoretical and Numerical Studies of Plume Flows in Vacuum Chambers," Ph.D. Dissertation, Department of Aerospace Engineering, Univ. of Michigan, Ann Arbor, MI, Oct. 2005.

[14] Cai, C., "Theoretical and Numerical Study of Several Free Molecular Flow Problems," 9th AIAA/ASME Joint Thermophysics and Heat Transfer Conference, San Francisco, CA, AIAA Paper 06-3800, 2006.

[15] Press, W. H., Vetterling, S. A., Flannery, W. T., and Flannery, B. P., *Numerical Recipes in C*, Cambridge Univ. Press, New York, 1994.

[16] Dietrich, S., and Boyd, I. D., "Scalar and Parallel Optimized Implementation of the Direct Simulation Monte Carlo Method," *Journal of Computational Physics*, Vol. 126, No. 2, July 1996, pp. 328–342.

A. Ketsdever
Associate Editor